

PHARMACEUTICS, PREFORMULATION AND DRUG DELIVERY

Intermolecular Contacts Influencing the Conformational and Geometric Features of the Pharmaceutically Preferred Mebendazole Polymorph C

FELIPE T. MARTINS,¹ PERSON P. NEVES,² JAVIER ELLENA,¹ GERARDO E. CAMÍ,³
ELENA V. BRUSAU,³ GRISELDA E. NARDA³

¹Physics Institute of São Carlos, University of São Paulo, CP 369, 13560-970 São Carlos, SP, Brazil

²Department of Exact Science, Federal University of Alfenas, 37130-000 Alfenas, MG, Brazil

³Química Inorgánica, Departamento de Química, Facultad de Química, Bioquímica y Farmacia, Universidad Nacional de San Luis, Chacabuco y Pedernera, 5700 San Luis, Argentina

Received 11 June 2008; revised 11 August 2008; accepted 3 September 2008

Published online 14 October 2008 in Wiley InterScience (www.interscience.wiley.com). DOI 10.1002/jps.21593

ABSTRACT: Mebendazole (MBZ) is a common benzimidazole anthelmintic that exists in three different polymorphic forms, A, B, and C. Polymorph C is the pharmaceutically preferred form due to its adequate aqueous solubility. No single crystal structure determinations depicting the nature of the crystal packing and molecular conformation and geometry have been performed on this compound. The crystal structure of mebendazole form C is resolved for the first time. Mebendazole form C crystallizes in the triclinic centrosymmetric space group and this drug is practically planar, since the least-squares methyl benzimidazolylcarbamate plane is much fitted on the forming atoms. However, the benzoyl group is twisted by $31(1)^\circ$ from the benzimidazole ring, likewise the torsional angle between the benzene and carbonyl moieties is $27(1)^\circ$. The formerly described bends and other interesting intramolecular geometry features were viewed as consequence of the intermolecular contacts occurring within mebendazole C structure. Among these features, a conjugation decreasing through the imine nitrogen atom of the benzimidazole core and a further resonance path crossing the carbamate one were described. At last, the X-ray powder diffractogram of a form C rich mebendazole mixture was overlaid to the calculated one with the mebendazole crystal structure. © 2008 Wiley-Liss, Inc. and the American Pharmacists Association *J Pharm Sci* 98:2336–2344, 2009

Keywords: crystallography; crystal structure; polymorphism; crystallization; X-ray powder diffractometry; mebendazole; polymorph C; benzimidazole derivative; anthelmintic drugs

INTRODUCTION

Mebendazole [(5-benzoyl-1*H*-benzimidazole-2-yl)-carbamic acid methyl ester, MBZ] is a potent, orally active, broad-spectrum anthelmintic which is intensively used in the treatment of ascariasis, uncinariasis, oxyuriasis, and trichuriasis. As with

Correspondence to: Felipe T. Martins (Telephone: 1633739333; Fax: 163372-2218; E-mail: felipetmartins@yahoo.com.br)

Journal of Pharmaceutical Sciences, Vol. 98, 2336–2344 (2009)
© 2008 Wiley-Liss, Inc. and the American Pharmacists Association

other benzimidazole anthelmintics, MBZ primary mechanism of action is consistent with tubulin binding.

MBZ belongs to class II of the biopharmaceutics classification systems (BCS), polymorphism studies being then essential for this compound. Several authors have investigated the polymorphism and physical stability of MBZ solid phases.^{1–3} Three polymorphic forms (A, B, and C) displaying significantly different solubilities and therapeutic effects have been identified and characterized.^{4,5} Diverse techniques have been applied to feature particular polymorphic forms in samples, infrared spectroscopy being the most commonly used method in the literature to identify MBZ solid state phases, whereas X-ray powder diffraction is preferred to quantify MBZ polymorphic mixtures and references.^{3,6,7}

Even though some discrepancies are reported in the literature concerning the relative solubility of forms B and C, all the authors agree that form A is the most abundant and stable and then the least soluble one.^{1,5} Thus, form C is pharmaceutically preferred since its solubility is enough to ensure optimal bioavailability without exhibiting the toxicity associated to form B.^{5,8,9} Furthermore, it was determined that at least 30% of form A in the formulation is enough to suppress the desirable pharmacological activity,^{10,11} thus indicating the high polymorphism dependence of the anthelmintic efficacy of MBZ.

Regarding physical properties, the three polymorphs have been mainly studied in relation to their thermal stability and dissolution behavior in several solvents. In addition, some MBZ solvates determined by single crystal X-ray diffraction have been reported. Mebendazole hydrobromide was found to crystallize in a monoclinic space group, $P2_1/c$,¹² whereas recrystallization of MBZ in propionic acid yields a 1:1 molecular complex crystallizing in the noncentrosymmetric triclinic space group, $P1$.¹³

Complete crystal structure data of MBZ polymorphs are not found in the literature because single crystals seem to be hard to obtain. In an attempt to obtain adequate crystals for single crystal X-ray diffraction we have recently reported a new stable salt, mebendazole hydrochloride which was also fully characterized by structural, vibrational and thermal analysis.¹⁴

In the present work we report the crystal structure solved by single crystal X-ray diffraction of MBZ C, which was obtained by recrystallization of the commercially available corresponding polymorph. Finally, the elucidation of the crystal

structure of MBZ form C can contribute to approach the crystal structures of forms A and B, that still remain unknown, and the structure–property relationships of MBZ will be stated.

EXPERIMENTAL

Materials and Preparation of MBZ Polymorph C

Polymorph C single crystals were obtained by recrystallization of microcrystalline MBZ C from methanol at 15°C. The methanolic solution (20 mg MBZ C in 100 mL) was let to stand in the dark for about 15 days until extremely thin, colorless prismatic crystals suitable for single crystal X-ray analysis were obtained. However, the crystals seem to be twinned by optical microscopy, due to the individual thin plates growing nearly. After the crystal structure solving, this mebendazole C behavior was related to its characteristic crystal packing. The mebendazole polymorph A was prepared from a glacial acetic acid solution according to a recrystallization protocol described in the literature.³ All used chemicals were of analytical grade. Concerning the X-ray powder diffraction analyses, the used samples, a raw material which is an MBZ form C rich mixture and a polymorph A sample, were obtained from the Instituto Nacional de Controle de Qualidade em Saúde, Fundação Oswaldo Cruz (FIOCRUZ, Manguinhos, Rio de Janeiro, Brazil), and from the Fundação Ezequiel Dias (FUNED, Gameleira, Belo Horizonte, Brazil), respectively. Both MBZ materials are certified as reference standard chemicals by the drug manufacturers. Nevertheless, the X-ray powder diffractograms of these samples were previously compared to that reported in the literature for the different MBZ polymorphs in order to ensure the expected contents.

Single Crystal X-Ray Diffraction Experiment

Recrystallizations of raw mebendazole (MBZ) in methanolic solution yielded a crystalline material, from which a well-shaped clear single crystal was selected for the X-ray diffraction experiment. Intensity data were collected at low temperature (150(2) K) kept by a cryogenic device (Oxford Cryosystem) and with graphite monochromated Mo K α radiation ($\lambda = 0.71073$ Å), using the *Enraf-Nonius Kappa-CCD* diffractometer. The cell refinements were performed using the software

Collect¹⁵ and Scalepack,¹⁶ and the final cell parameters were obtained on all reflections. Data for MBZ were measured up to 50.90° in 2 θ , totaling 4498 Bragg reflections. Data reduction was carried out using the software Denzo-SMN and Scalepack¹⁵ and XdisplayF for visual representation of data. A negligible absorption coefficient of 0.103 mm⁻¹ was observed. Although the International Union of Crystallography (IUCr) states that there is no need of absorption correction if the product μx , where μ is the absorption coefficient value (0.103 mm⁻¹) and x is the medial crystal size (0.10 mm for the measured MBZ crystal, Tab. 1), is below 0.1,¹⁷ trial refinements were employed considering this procedure. However, significant statistical improvements were not obtained and we have preferred to comply with IUCr recommendations, ruling out the absorption correction since the product μx was 0.0103 for the experimented mebendazole C crystal.

The structure was solved using SHELXS-97¹⁸ and refined using SHELXL-97 software.¹⁹ The C, N, and O atoms were clearly solved and full-matrix least-squares refinement of these atoms with anisotropic thermal parameters was carried out. The C–H hydrogen atoms were positioned stereochemically and were refined

with fixed individual displacement parameters [$U_{\text{iso}}(\text{H}) = 1.2U_{\text{eq}}(\text{C}_{\text{sp}}^2)$ or $1.5U_{\text{eq}}(\text{C}_{\text{sp}}^3)$] using a riding model with aromatic C–H bond length of 0.95 Å and methyl C–H one of 0.98 Å. The amine H atoms were located by difference Fourier analysis and were set as isotropic ($U_{\text{iso}}(\text{H}) = 1.2U_{\text{eq}}(\text{N})$). Wherefore, the positional parameters of these H atoms were not constrained during refinements. An attempt was made to consider the twinning with the ROTAX procedure, which is able to identify possible twin laws using trends in the indices of the poorly agreeing data group wherein the observed structure factor values are quite greater than the calculated ones.²⁰ The twin orientation matrix and the refined twin ratio (defined as the fractional contribution of each twin component) allowing the structure solving are found to be (100, 1, -1, 0, 1, 0, -1) and 0.17, respectively.

Table 1 presents a summary of data and structure refinement that was prepared with WinGX (version 1.70.01).²¹ ORTEP-322 and MERCURY23 were also used in order to prepare the crystal data for publication, as well as the MOGUL,²² a useful program to check the molecular conformation and geometry. This last tool performs substructure searches for chemicals

Table 1. Crystal Data and Structure Refinement for Mebendazole (MBZ)

Empirical formula	C ₁₆ H ₁₃ N ₃ O ₃
Formula weight	295.29
Temperature (K)	150(2)
Wavelength (Å)	0.71073
Crystal system	Triclinic
Space group	<i>P</i> -1
Unit cell dimensions	$a = 5.1480(9)$ Å, $b = 7.8779(15)$ Å, $c = 17.907(3)$ Å, $\alpha = 82.425(6)^\circ$, $\beta = 82.743(7)^\circ$, $\gamma = 71.091(13)^\circ$
Volume (Å ³)	678.3(2)
<i>Z</i>	2
Density (calculated) (Mg/m ³)	1.446
Absorption coefficient (mm ⁻¹)	0.103
<i>F</i> (000)	308
Crystal size (mm)	0.25 × 0.10 × 0.05
θ -Range for data acquisition (°)	4.20–25.45
Index ranges	$-6 \leq h \leq 5$, $-9 \leq k \leq 9$, $-21 \leq l \leq 21$
Reflections collected	4498
Independent reflections	2434 [$R(\text{int}) = 0.1502$]
Completeness to $\theta = 25.45^\circ$	96.7%
Refinement method	Full-matrix least-squares on F^2
Data/restraints/parameters	2434/0/207
Goodness-of-fit on F^2	1.348
Final <i>R</i> for $I > 2\sigma(I)$	$R1 = 0.1325$
<i>R</i> for all data	$wR2 = 0.4089$
Largest diff. peak and hole (e.Å ⁻³)	0.281 and -0.373

deposited at Cambridge Crystallographic Data Centre (CCDC)²³ that are composed of moieties similar to those of the query compound inputted either manually or by another computer software via an instruction-file interface.

The crystallographic information file (CIF) loading the data sets (excluding the structure factors) for MBZ form C has been deposited with the Cambridge Structural Data Base under deposit code CCDC 690724 (copies of these data may be obtained free of charge from The Director, CCDC, 12 Union Road, Cambridge CB2 1EZ, UK, fax: +44-123-336-033; e-mail: deposit@ccdc.cam.ac.uk or <http://www.ccdc.cam.ac.uk>).

X-Ray Powder Diffraction (XRPD) Matching

The X-ray patterns of the mebendazole raw material, a form C rich mixture of polymorphs A and C, and form A were recorded at room temperature (293 K) on a Rigaku Denki diffractometer using Cu K α radiation ($\lambda = 1.5418 \text{ \AA}$), 50 kV and 400 mA generator settings, RINT2000 wide angle goniometer and continuous scan mode. The samples were finely ground, mounted on a grooved glass slide employed as sample holder and exposed to the X-ray beam with scan speed 1.000 $^\circ/\text{min}$, sampling width 0.020 $^\circ$, scan axis $\theta - 2\theta$, 2θ range 3–40 $^\circ$. It is key to highlight that polymorphic transformations surely did not occur due to grinding procedure and that significant particle-size effects were not observed in the powder diffraction patterns; the measured diffractograms of a form A sample and raw material are in good agreement with those reported in the literature.³ Furthermore, there is a need of a simple care not to introduce a preferred orientation of MBZ crystals.³

The experimental X-ray powder diffraction (XRPD) patterns of mebendazole raw material and polymorph A were indexed with the data base PDF-2 Release 2006 (International Center for Diffraction Data[®]-ICDD), entries number 00-039-1606, 00-037-1627, and 00-034-1570 utilizing the program MATCH! a software for phase identification from X-ray powder diffraction data.²⁴

The theoretical XRPD peak positions were simulated with MERCURY²⁵ inputting the MBZ CIF file created after the structure refinement has been finalized. The unit cell parameters from the single crystal structure were slightly adjusted with the use of PowderCell software,²⁶ in an attempt to avoid bias due to the temperature discrepancy between the experimental powder analysis (room temperature) and single crystal measurements

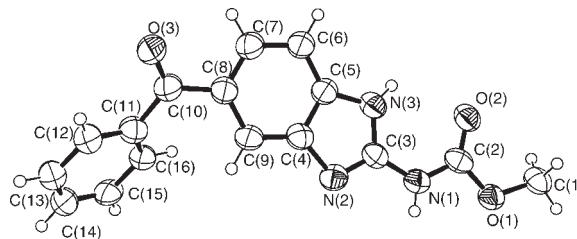


Figure 1. The ORTEP view of MBZ. Ellipsoids represent 50% probability level and an atom labeling scheme is arbitrarily adopted. The hydrogen atoms are shown as spheres of arbitrary radii.

(150 K). Afterwards, the subtly shifted X-ray diffraction peak positions from the crystal structure were then used for comparisons with the experimental X-ray powder diffractograms, which were also performed with PowderCell.²⁶

RESULTS AND DISCUSSION

The asymmetric unit of MBZ is depicted in Figure 1, an ORTEP-3 view.²⁷ Among all the likely tautomeric forms illustrated in Figure 2 for MBZ, it was concluded by XRD analysis that tautomer MBZ1 is predominant in the crystalline state. Such specific tautomer plays a decisive role in the crystal packing due to its intermolecular hydrogen bond pattern. As it can be seen in Table 2, where the details of the classical and nonclassical hydrogen-bond contacts in the network of MBZ are presented, and Figure 3 exhibiting the solid-state packing representation of MBZ onto the plane (123), a strong intermolecular hydrogen bond involving the atoms N(1)–H(1)···N(2) contacts two inversely related molecules in the lattice to form a dimer in which the nitrogen atom of the carbamate moiety is the hydrogen donor and the imine nitrogen one of the benzimidazole group is the acceptor. Into this same plane, the dimers are bonded to each other by a weak nonclassical hydrogen bond involving the atoms C(6)–H(6)···O(2), which gives rise to the infinite one-dimensional chains along the [2,–1,–3] direction (Tab. 2). These chains form stacked plane layers that explain the crystal morphology in aggregated thin plates and the tendency for the lattice twinning. Furthermore, the crystal structure solving and the final R factors of the refinement were just possible if a twinned structure model is taken, as it was described in the Experimental part. The previous

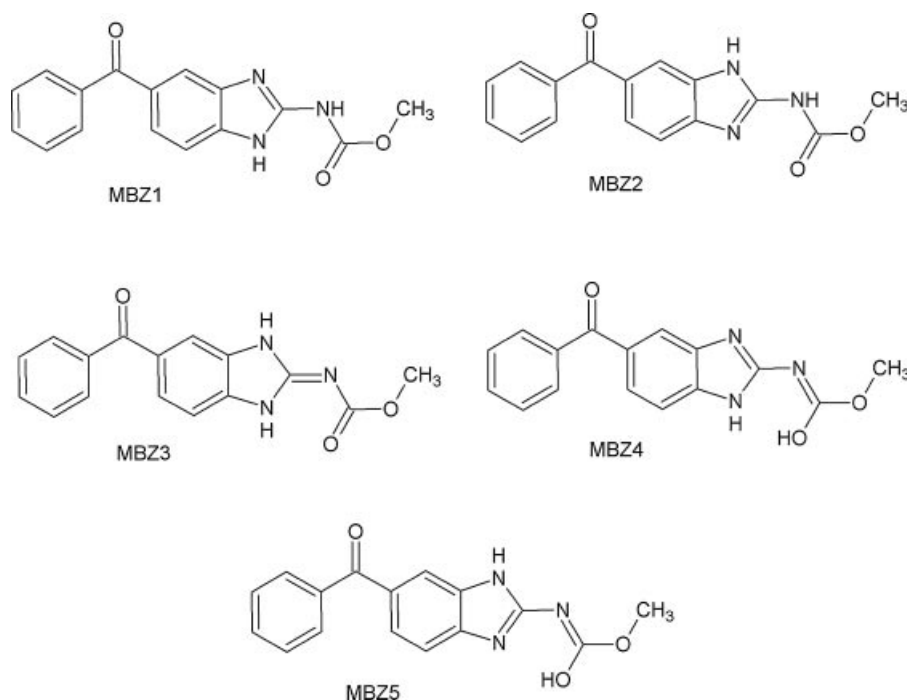


Figure 2. Tautomers of MBZ. The XRD structural determination has proved to be the tautomeric form MBZ1 present in the polymorph C crystal.

contact is shown in Figure 4, together with the nonclassical C(1)–H(1C)···O(3) H-bond connecting the 3.5 Å distanced parallel layers (Fig. 5). Another important interaction between two molecules of adjacent layers is the charge transfer from electron-rich C(6) carbon atom of the benzimidazolyl group to the electronically depleted C(2) one of the carbamate moiety. A key observation provides evidence for this contact and its importance for crystal packing: the geometry of the sp^2 -hybridized C(6) carbon atom is partially tetrahedral as result of the intermolecular bond formation between C(2) and C(6), which can be affirmed accounting the marked contraction of the valence angle C(5)–C(6)–C(7) ($115.4(7)^\circ$). An

expected corresponding value for a perfect trigonal geometry is $120(2)^\circ$, as it was found by MOGUL analysis of 1160 hits in CSD.

The O(2) oxygen atom also acts as an intramolecular hydrogen acceptor from the amine N(3)–H(3) group present in the benzimidazole core (Tab. 2, Fig. 3). The classical moderate N(3)–H(3)···O(2) hydrogen bond closes a chelating six-membered system composed by O(2)–C(2)–N(1)–C(3)–N(3)–H(3) atoms. The highest deviation from the least-squares plane passing through the six cyclic atoms above mentioned is 0.11(3) Å for H(3) (root mean square deviation (r.m.s.d.) of fitted atoms is 0.0636 Å), showing that such system is appreciably planar. However, since the

Table 2. Hydrogen-Bonding Geometry (Å, °) for MBZ

D–H···A	D–H	H···A	D···A	D–H···A
N(3)–H(3)···O(2)	0.82(9)	2.31(7)	2.720(9)	112(6)
N(1)–H(1)···N(2) ^a	0.81(7)	2.09(7)	2.877(9)	165(6)
C(6)–H(6)···O(2) ^b	0.95	2.51	3.35(1)	147
C(1)–H(1C)···O(3) ^c	0.98	2.70	3.56(1)	147

The symbols “D” and “A” mean hydrogen donor and acceptor, respectively.

^aSymmetry: $-x, 1-y, -z$.

^bSymmetry: $2-x, -y, -z$.

^cSymmetry: $1-x, -y, -z$.

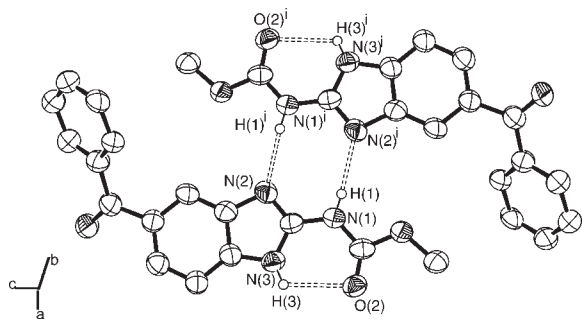


Figure 3. MBZ dimer projected onto the plane (123) showing the strong intermolecular N(1)–H(1)···N(2) hydrogen bond connecting the molecules, likewise the moderate intramolecular N(3)–H(3)···O(2) interaction can be evidenced. Double dotted lines illustrate the hydrogen bonds. The H-atoms involved in the hydrogen bonds are shown as spheres of arbitrary radii. Symmetry code: (i) $-x; 1-y; -z$.

noncovalent interaction between the amine and carbonyl groups is not strong (N(3)···O(2) separation and the N(3)–H(3)···O(2) angle are 2.720(9) Å and 112(6)°, respectively), a planarity decrease was already expected in a chelating ring wherein an amine sp^3 -hybridized nitrogen atom, the N(3), is present. The highest deviation from the least-squares plane fitted on this cycle for H(3) hydrogen atom reveals that the geometry of the nitrogen atom bonded to it, N(3), lies between trigonal-planar and trigonal-pyramidal, distorting slightly the planarity of the intramolecularly hydrogen bonded system. Furthermore, this chelating system is also weakened because the intermolecular C(6)–H(6)···O(2) hydrogen bonding contributes to take the carbonyl O(2) oxygen atom away from the six-membered moiety.

The carbonyl group of the benzoyl moiety is twisted from the benzimidazole plane, which can be noted by looking at the C(7)–C(8)–C(10)–O(3) torsional angle value, 31(1)°, a value that is significantly greater than expected for a perfectly conjugated π -system, about 0°. Similarly, the carbonyl group is noncoplanar with the phenyl ring, since the dihedral angle C(12)–C(11)–C(10)–O(3) measures 27(1)° instead 0°, an approximate value that is required to consider them as coplanar. Strengthening the statement concerning the absence of planarity between the carbonyl bridge and the two cyclic systems bonded to it, the O(3) oxygen atom deviates 0.60(1) and 0.61(1) Å from the least-squares benzimidazole and phenyl planes, respectively. Therefore, there are no resonance effects between the C(10)=O(3) carbonyl and benzimidazolyl groups, likewise this carbonyl motif is not conjugated with the phenyl one. A cause for these interesting conformational features is in the occurrence of the intermolecular C(1)–H(1C)···O(3) hydrogen bonding that bends the O(3) oxygen atom to accept the donated hydrogen by the side chain methyl group of a adjacent molecule packed along the layer overlapping direction [123]. Indeed, the C(10)=O(3) carbonyl twisting is a consequence of the C(1)–H(1C) hydrogen donor pulling the O(3) oxygen atom to optimize the hydrogen bond orientation.

The determined intramolecular geometry of compound MBZ was analyzed using MOGUL,²² and all bond angles and distances are in agreement with what is expected for good structural solving and refinement. However, the MOGUL evaluation showed some notable deviations from the expected values for intramolecular bond distances that can be rationalized taking in

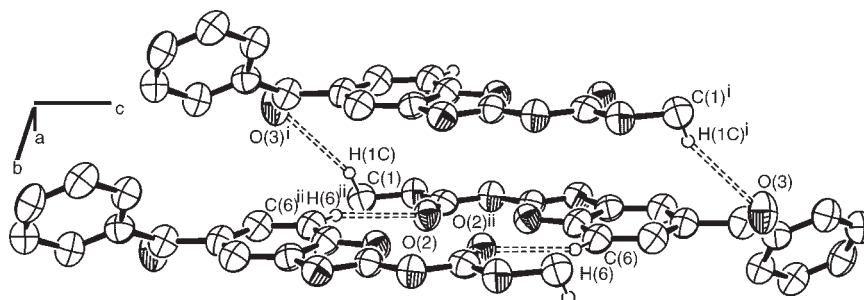


Figure 4. Weak nonclassical hydrogen bonds contributing to MBZ crystal packing along the directions [123] (symmetry operator: (i) $1-x; -y; -z$) and $[2, -1, -3]$ (symmetry operator: (ii) $2-x; -y; -z$). Double dotted lines represent the intermolecular hydrogen bonds. The H-atoms involved in the hydrogen bonds are shown as spheres of arbitrary radii.

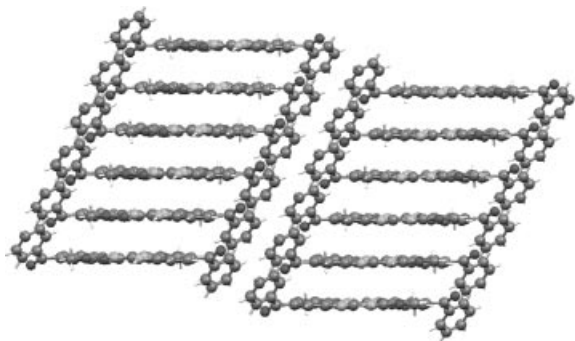


Figure 5. Mebedazole layers separated by 3.5 Å in the polymorph C crystal packing.

account the influence of the intermolecular contacts on the MBZ electronic properties. The N(2) nitrogen atom accepting hydrogen in the strong intermolecular N(1)–H(1)··N(2) interaction has its free electron pair hindered to be donated to the C(4) carbon atom in a resonance path passing through the benzimidazole ring, once these two electrons are directly implicated in the hydrogen acceptance from the amide N(1)–H(1) group. So, the conjugation is decreased through the N(2) nitrogen and carbon atoms bonded to it, C(3) and C(4). The detached double

bond character of the N(2)=C(3) binding (1.30(1) Å) and the N(2)–C(4) one (1.42(1) Å) with an enhanced single bond feature have allowed us to get this insight, since the N(2)=C(3) distance is markedly shorter than the average value in query, 1.33(2), and the single bond N(2)–C(4) is longer than the measurement 1.39(2) Å averaged on 1266 MBZ-like compounds returned by MOGUL surveys in the Cambridge Structural Database (CSD).²³ In Figure 6, a MOGUL histogram exhibits the comparison of the N(2)–C(4) single bond distance with equivalent N–C bond lengths of MBZ-like structures deposited in the CSD. In an opposed behavior, the mono-substituted amide N(1) nitrogen has a tendency to conjugate the free electrons since this atom is a hydrogen donor in the N(1)–H(1)··N(2) intermolecular interaction. In this way, a further conjugated system occurs through the carbamate moiety, which was revealed by the double bond feature of the single N(1)–C(2) bond that is shortened in MBZ (1.33(1) Å compared to a MOGUL mean value of 1.37(2) Å).

Regarding the polymorphism of MBZ, at least three true polymorphs are known to exist, that is, crystalline forms A, B, and C.^{4,7} In this context, we have analyzed samples of purified form A and polymorph C rich mixture by X-ray powder diffraction (XRPD) at room temperature to

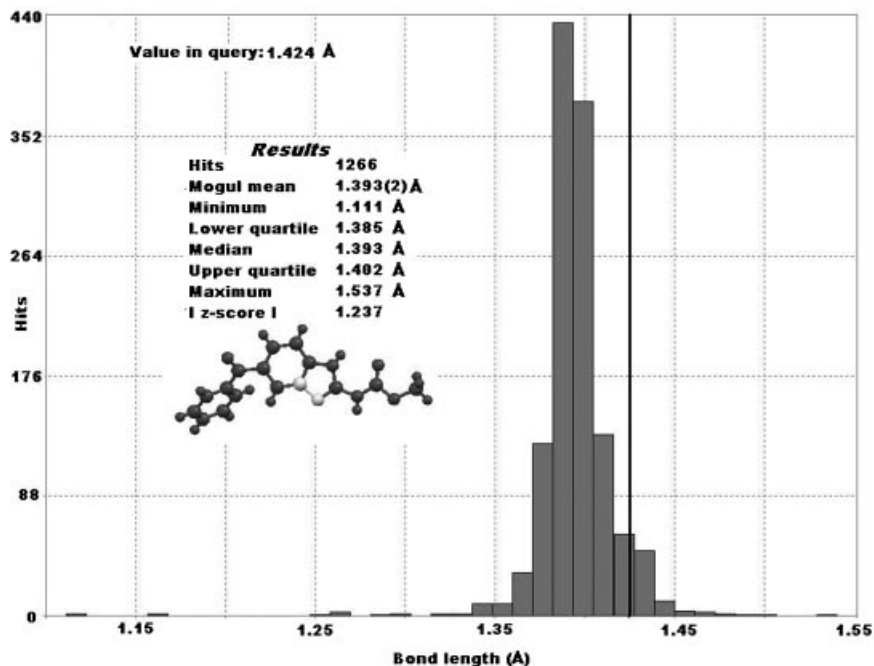


Figure 6. Histogram comparing the N(2)–C(4) bond length of MBZ with the equivalent distances of resembled compounds found in CSD.

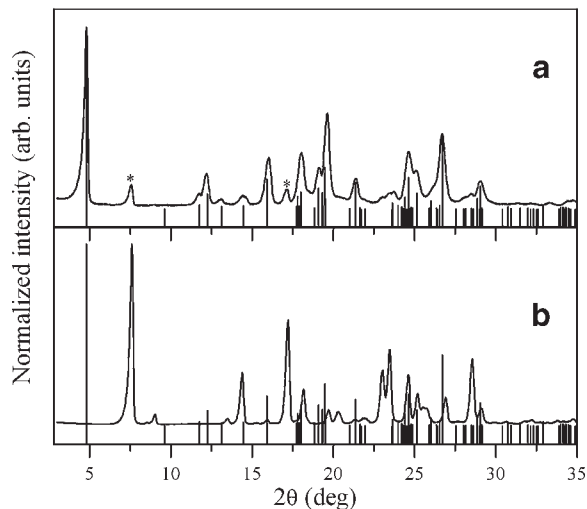


Figure 7. Comparison among the X-ray powder peak positions from MBZ single crystal structure (vertical bars) and diffractograms (full line) of a form C rich mixture containing the mebendazole polymorphs A and C (a) and raw mebendazole polymorph A (b). The asterisks represent the most intense Bragg reflections of phase A that appear in the form C rich mixture.

identify which one was determined using single crystal X-ray diffraction. After the structure refinement end, an MBZ CIF file was then generated. From this file, the theoretical XRPD peak positions were simulated with MERCURY.²³ They were compared with the experimental diffractograms of: (a) a mixture of MBZ forms A and C containing the polymorph C in higher proportion (Fig. 7a), and (b) a pure polymorph A sample (Fig. 7b). All simulated diffraction peaks were overlaid to those of the form C rich mixture diffractogram. Just two Bragg reflections detected in the mixture XRPD profile were absent in the theoretical diffractogram. These diffraction peaks are the most intense ones of phase A (asterisk marked). It is important to emphasize that MBZ crystal transformations do not occur at low temperatures³ and therefore the calculated XRPD peak positions have been fitted with PowderCell program²⁶ by adjusting the crystallographic unit cell parameters. With this procedure, peak position discrepancies potentially caused by temperature differences (crystal structure diffractogram is at 150 K and the experimental measurements are at 293 K) are avoided. Concluding, the XRPD profile matching has assigned the MBZ single crystal structure determined here to be the pharmaceutically preferred form C.

CONCLUSIONS

The crystal structure of mebendazole polymorph C was determined for the first time in this work, resulting in a complete characterization of intra- and inter-molecular geometries. In the solid state of mebendazole form C, the featured tautomer shows an intermolecular contact pattern with nonclassical and classical hydrogen bonds, including a strong hydrogen bond involving the amide and imine groups of the carbamate and benzimidazole moieties, respectively. Such intermolecular interaction connects two inversely related molecules to form dimers that are repeated infinitely into layers hydrogen bonded by the methyl group and carbonyl one of the benzoyl portion. Furthermore, the supramolecular assembly noncovalent bonds have influenced the mebendazole C electronic properties and structure conformation. The availability of this full crystallographic analysis let us to go deeper into the vibrational–structural relationship of MBZ C. Additionally, a more reliable assignment of the IR and Raman spectra is currently on progress.

ACKNOWLEDGMENTS

The authors thank CNPq (CNPQ), FAPESP (F.T.M.) and FAPEMIG (P.P.N.) for research fellowships, the CONICET: PID 6246/05 and UNSL (Argentina) for financial support. G.E.N. is member of the CONICET.

REFERENCES

- Swanepoel E, Liebenberg W, de Villiers MM. 2003. Quality evaluation of generic drugs by dissolution test: Changing the USP dissolution medium to distinguish between active and non-active mebendazole polymorphs. *Eur J Pharm Biopharm* 55:345–349.
- Swanepoel E, Liebenberg W, Devarakonda B, de Villiers MM. 2003. Developing a discriminating dissolution test for three mebendazole polymorphs based on solubility differences. *Pharmazie* 58:117–121.
- de Villiers MM, Terblanche RJ, Liebenberg W, Swanepoel E, Dekker TG, Song M. 2005. Variable-temperature X-ray powder diffraction analysis of the crystal transformation of the pharmaceutically preferred polymorph C of mebendazole. *J Pharm Biomed Anal* 38:435–441.

4. Himmelreich M, Rawson BJ, Watson TR. 1977. Polymorphic forms of mebendazole. *Aust J Pharm Sci* 6:123–125.
5. Rodriguez-Caabeiro F, Criado-Fornelio A, Jimenez-Gonzalez A, Guzmán L, Igual A, Pérez A, Pujol M. 1987. Experimental chemotherapy and toxicity in mice of three mebendazole polymorphic forms. *Chemotherapy* 33:266–271.
6. Aboul-Enein HY, Bunaciu AA, Fleschin S. 2002. Analysis of mebendazole polymorphs by Fourier Transform IR spectrometry using chemometric methods. *Biopol Biospectrosc* 67:56–60.
7. Liebenberg W, Dekker TG, Lotter AP, de Villiers MM. 1998. Identification of Mebendazole polymorphic form present in raw materials and tablets available in South Africa. *Drug Dev Ind Pharm* 24:485–488.
8. Charoenlarp P, Waikagul J, Muennoo C, Srinophakun S, Kitayaporn D. 1993. Efficacy of single-dose mebendazole, polymorphic forms A and C, in the treatment of hookworm and *Trichuris infections*. *Southeast Asian J Trop Med Public Health* 24:712–716.
9. Costa J, Fresno M, Guzmán L, Igual A, Oliva J, Vidal P, Pérez A, Pujol M. 1991. Polymorphic forms of mebendazole: Analytical aspects and toxicity. *Circ Farm* 49:415–424.
10. Evans AC, Fincham JE, Dhansay MA, Liebenberg W. 1999. Anthelmintic efficacy of mebendazole depends on the molecular polymorph. *S Afr Med J* 89:1118.
11. Ren H, Cheng B, Ma J, Hua D. 1987. Comparative effectiveness of mebendazole with different polymorphic forms against *nippostrongylus braziliensis*. *Yiyao Gongye* 18:356–3359.
12. Blaton NM, Peeters OM, De Ranter CJ. 1980. (5-benzoyl-1H-benzimidazol-2-yl)-carbamic acid methyl ester hydrobromide (Mebendazole.HBr), $C_{16}H_{14}BrN_3O_3$. *Cryst Struct Comm* 9:181–186.
13. Caira MR, Dekker TG, Liebenberg W. 1998. Structure of a 1:1 complex between the anthelmintic drug mebendazole and propionic acid. *J Chem Crystallogr* 28:11–15.
14. Brusau EV, Camí GE, Narda GE, Cuffini S, Ayala AP, Ellena J. 2008. Synthesis and characterization of a new mebendazole salt: Mebendazole hydrochloride. *J Pharm Sci* 97:542–552.
15. Enraf-Nonius 1997–2000. COLLECT Nonius BV, Delft, The Netherlands.
16. Otwinowski Z, Minor W. 1997. Processing of X-ray diffraction data collected in oscillation mode. HKL Denzo and Scalepack. *Methods in Enzymology* 276:307–326. In: Carter CW Jr., Sweet RM, editors. *Macromolecular Crystallography, Part A*. New York: Academic Press.
17. International Union of Crystallography. 2008. Notes for Authors. *Acta Crystallogr. Sect C* 64: e2–e9.
18. Sheldrick GM. 1997. SHELXS97 Program for Crystal Structure Resolution, University of Göttingen, Germany.
19. Sheldrick GM. 1997. SHELXL97 Program for Crystal Structures Analysis, University of Göttingen, Germany.
20. Cooper RI, Gould RO, Parsons S, Watkin DJ. 2002. The derivation of non-merohedral twin laws during refinement by analysis of poorly fitting intensity data and the refinement of non-merohedrally twinned crystal structures in the program CRYSTALS. *J Appl Crystallogr* 35:168–174.
21. Farrugia LJ. 1999. WinGX suite for small-molecule single-crystal crystallography. *J Appl Crystallogr* 32:837–838.
22. Bruno IJ, Cole JC, Kessler M, Luo J, Motherwell WDS, Purkis LH, Smith BR, Taylor R, Cooper RI, Harris SE, Orpen AG. 2004. Retrieval of crystallographically-derived molecular geometry information. *J Chem Inf Comput Sci* 44:2133–2144.
23. Allen FH. 2002. The Cambridge Structural Database: A quarter of a million crystal structures and rising. *Acta Crystallogr Sect B* 58:380–388.
24. Brandenburg K, Putz H. MATCH!, version 1.8, Crystal Impact, Bonn, Germany.
25. Bruno IJ, Cole JC, Edgington PR, Kessler MK, Macrae CF, McCabe P, Pearson J, Taylor R. 2002. New software for searching the Cambridge Structural Database and visualizing crystal structures. *Acta Crystallogr Sect B* 58:389–397.
26. Kraus W, Nolze G. PowderCell for Windows, version 2.3, Federal Institute for Materials Research and Testing, Berlin, Germany.
27. Farrugia LJ. 1997. ORTEP-3 for Windows—A version of ORTEP-III with a Graphical User Interface (GUI). *J Appl Crystallogr* 30:565.